Escherichia coli Uracil DNA Glycosylase: NMR Characterization of the Short Hydrogen Bond from His187 to Uracil O2[†]

Alexander C. Drohat and James T. Stivers*

Center for Advanced Research in Biotechnology of the National Institute of Standards and Technology and the University of Maryland Biotechnology Institute, 9600 Gudelsky Drive, Rockville, Maryland 20850

Received April 24, 2000

ABSTRACT: Uracil DNA glycosylase (UDG) cleaves the glycosidic bond of deoxyuridine in DNA using a hydrolytic mechanism, with an overall catalytic rate enhancement of 10^{12}-fold over the solution reaction. The nature of the enzyme−substrate interactions that lead to this large rate enhancement are key to understanding enzymatic DNA repair. Using ^{1}H and heteronuclear NMR spectroscopy, we have characterized one such interaction in the ternary product complex of *Escherichia coli* UDG, the short (2.7 Å) H bond between His187 $N^{\epsilon 2}$ and uracil O2. The H bond proton is highly deshielded at 15.6 ppm, indicating a short N-O distance and exhibits a solvent exchange rate that is 400- and 10^5-fold slower than free imidazole at pH 7.5 and pH 10, respectively. Heteronuclear NMR experiments at neutral pH show that this H bond involves the neutral imidazole form of His187 and the N1-O2 imidate form of uracil. The excellent correspondence of the pK_a for the disappearance of the H bond (p$K_a = 6.3 \pm 0.1$) with the previously determined p$K_a = 6.4$ for the N1 proton of enzyme-bound uracil indicates that the H bond requires negative charge on uracil O2 [Drohat, A. C., and Stivers, J. T. (2000) *J. Am. Chem. Soc. 122,* 1840−1841]. Although the above characteristics suggest a short strong H bond, the D/H fractionation factor of $\phi = 1.0$ is more typical of a normal H bond. This unexpected observation may reflect a large donor−acceptor pK_a mismatch or the net result of two opposing effects on vibrational frequencies: decreased N-H bond stretching frequencies ($\phi < 1$) and increased bending frequencies ($\phi > 1$) relative to the O-H bonds of water. The role of this H bond in catalysis by UDG and several approaches to quantify the H bond energy are discussed.

One component of the tremendous catalytic power of enzymes is their capacity to stabilize charge reorganization in the transition state to a much greater extent than can occur in solution. This fundamental property of enzymes can be partially attributed to their preorganized active sites, which are complementary to the electronic features of the substrate in its transition-state conformation (*1*, *2*) and to the enhanced strength of electrostatic interactions in the active-site environment as compared to water (*3*). Despite general agreement on the importance of these effects, the nature and strength of the electrostatic interactions used by enzymes to preferentially stabilize the transition-state is still the subject of much investigation and debate (*1*, *2*, *4*).

A deceptively simple interaction that an enzyme can form to stabilize a negatively charged transition state is a hydrogen bond (H bond). It has been proposed that under certain conditions enzymes can form unusually short, strong, or low-barrier H bonds (SSHB or LBHB) to stabilize charge development in the transition state by up to 84 kJ/mol (20 kcal/mol) (*5*−*7*). An LBHB differs from a normal H bond in that the double-well potential energy surface has a small barrier for transfer of the proton, which requires closely matched pK_a values for the donor and acceptor (*8*). Although the energetic barrier for proton transfer in a SSHB is greater, there is a smooth energetic transition from the SSHB to the LBHB as the pK_a difference between the donor−acceptor pair is reduced (*3*, *9*). However, the existence and energetic contribution of LBHBs in enzymatic catalysis has been challenged on theoretical and computational grounds (*10*−*13*) and on the basis of experimental observations (*14*). An alternative proposal is that simple electrostatic stabilization, in combination with a preorganized active site of low effective dielectric, is sufficient to account for the rate enhancements observed for many enzymes (*1*−*3*, *15*, *16*).

We have recently established an electrophilic role in catalysis for the active-center histidine of the DNA repair enzyme uracil DNA glycosylase (UDG) (*17*, *18*). This enzyme catalyses the hydrolysis of the *N*-glycosidic bond of premutagenic deoxyuridine (dU) residues in DNA by flipping dU from the DNA, producing uracil and abasic DNA (*19*−*21*). During the course of this reaction, negative charge develops on the uracil base that must be accommodated by the active site environment of the enzyme. Recent mutagenesis, kinetic, and heteronuclear NMR experiments indicate that *Escherichia coli* UDG stabilizes the developing negative charge by providing an H bond from a neutral His187 to uracil O2 that is worth about 20 kJ/mol in the transition state (*17*, *18*). More recent heteronuclear NMR experiments have revealed, much to our surprise, that the uracil base is anionic

[†] This work was supported by NIH Grant GM56834 (J.T.S.) and the National Institute of Standards and Technology. A.C.D. is a National Research Council Postdoctoral Associate.

* To whom correspondence should be addressed. Phone: (301) 738-6264; fax: (301) 738-6255; e-mail: stivers@carb.nist.gov.

10.1021/bi000922e CCC: $19.00
Published on Web 09/02/2000

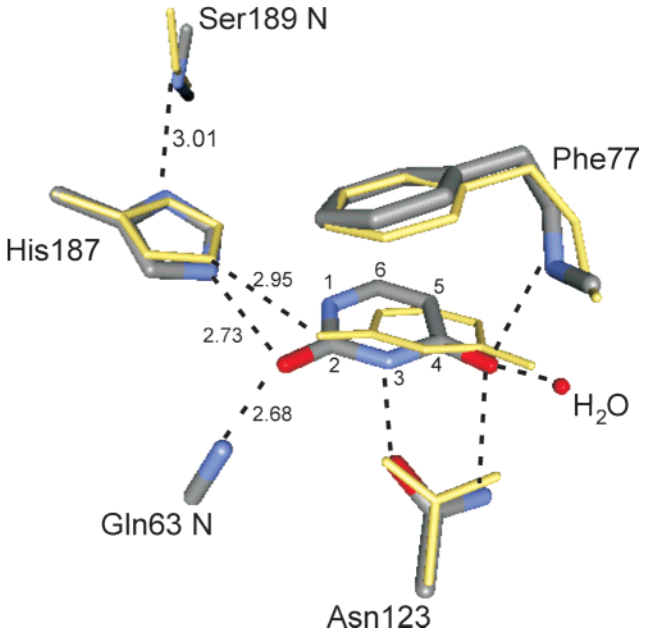

FIGURE 1: Uracil binding pocket from the product complex of human UDG with duplex AB DNA [colored by atom type (*20*)] superimposed with that of *E. coli* UDG and single stranded AB DNA [yellow, (*58*)]. The H bonds to uracil O2, N3, and O4 are indicated by dashed lines, and donor−acceptor distances (Å) are given for the H bonds to O2. The residue numbering is for *E. coli* UDG, and the uracil atoms are numbered for clarity.

and in the N1-O2 imidate form in the ternary product complex at neutral pH ($pK_a^{N1} = 6.4 \pm 0.1$) (*22*) (Figure 1). This key observation shows that the enzyme stabilizes the uracil anion by a surprising 3.4 units as compared to free uracil ($pK_a^{N1} = 9.8$) (*23*), corresponding to 20 kJ/mol of stabilization energy by the enzyme. This observation indicated that the ternary product complex of UDG with abasic DNA and uracil is a stable approximation for the ionic transition state of the UDG reaction that could be studied using NMR methods.

In this paper, we show that the H bond between His187 and the uracil O2 anion in the UDG product complex has many of the characteristics of a short strong H bond, such as that found in the active sites of serine proteases and isomerase enzymes (*24*−*26*). These results provide further evidence for the ubiquitous nature of these interactions in enzymology. To the best of our knowledge, this is the first observation of such an H bond in a DNA repair enzyme.

EXPERIMENTAL PROCEDURES[1]

Materials. Wild-type and 6X-amino terminal His-tagged H187G and H187Q UDG from *E. coli* strain B were produced using a T7 polymerase-based expression system and purified to >99% homogeneity as described (*18*, *19*). Uniformly ^{15}N-labeled UDG was prepared as described (*17*). The oligodeoxynucleotides were synthesized, purified, and characterized essentially as described (*21*) including characterization by MALDI-TOF[2] mass spectrometry. The oligonucleotide containing the AB site was 5′-GCGCA**X**-AGTCG-3′, where **X** denotes the AB site, and the complementary strand for the dsAB DNA was 5′-CGACTATGCGC-3′. The dsAB and ssAB DNA used in these studies contained a tetrahydofuran AB-site analogue (Glen Research, Sterling, VA). Although this analogue differs slightly from the AB site of the natural product in that a 1′-hydrogen replaces the 1′-hydroxyl group, the same highly deshielded resonance arising from the hydrogen bond between His187 and uracil O2 is observed for the ternary product complex formed with both types of AB sites (not shown). The duplex DNA was hybridized as previously described (*21*), except that the buffer was 10 mM NaH_2PO_4 (pH 7.5) and 100 mM NaCl. The D_2O (99.9 atom % D) and DMSO-d_6 (99.9 atom % D) were from Cambridge Isotope Labs (Andover, MA). The [^{13}C]-2-labeled uracil was from Isotech, Inc. (Miamisburg, OH). The components of the NMR samples were treated with Chelex 100 resin (iminodiacetic acid, Sigma, St. Louis, MO) to remove paramagnetic impurities.

Dissociation Constant for Uracil Binding. The apparent dissociation constants (K_D^{app}) for the binding of uracil to UDG (Figure 8) were determined by titrating fixed concentrations of UDG (1 to 20 μM) with increasing amounts of uracil and monitoring the tryptophan fluorescence of the enzyme (*21*). An excitation wavelength of 290 nm was used to minimize the absorption of uracil, and emission spectra in the range of 315 to 450 nm were collected. The fluorescence intensity at 330 nm was used in the K_D^{app} calculations after correction for absorption of the excitation beam by uracil, i.e., the primary absorption or inner-filter effect (*27*). The binding data were fitted to eq 1 using Grafit 4.0 (*28*):

$$F = F_o - \{(F_o - F_f)/2 \times [UDG]_{tot}\} \times \{b - (b^2 - 4[UDG]_{tot}[uracil]_{tot})^{1/2}\} \quad (1)$$

where F_o and F_f are the initial and final fluorescence intensities and $b = K_D^{app} + [UDG]_{tot} + [uracil]_{tot}$. The buffers used for the different pH values were (all 10 mM): NaH_2PO_4, pH 6.45; Tris-HCl; pH 7.1 to pH 8.0; NaCHES, pH 8.5 to 9.5; NaCAPS, pH > 9.5. The $MgCl_2$ concentration was 2.5 mM, and the NaCl concentration was 20 mM.

General NMR Spectroscopy. NMR experiments were conducted on Bruker DRX500 or DRX600 spectrometers, each equipped with four frequency channels and a triple-axis gradient $^1H-^{13}C-^{15}N$ probe. Proton chemical shifts are reported with respect to external DSS in the buffer used for most of the NMR experiments (10 mM NaH_2PO_4, pH 7.5, and 250 mM NaCl). The ^{13}C and ^{15}N chemical shifts were indirectly referenced to DSS and liquid NH_3, respectively, using the zero point frequency ratios $^{13}C/^1H = 0.251449530$ and $^{15}N/^1H = 0.101329118$ (*29*). Experiments were conducted with 1-s recycle delays unless stated otherwise. The

[1] Certain commercial equipment, instruments, and materials are identified in this paper to specify the experimental procedure. Such identification does not imply recommendation or endorsement by the National Institute of Standards and Technology, nor does it imply that the material or equipment identified is necessarily the best available for the purpose.

[2] Abbreviations: AB, abasic; dsAB, duplex abasic 11-mer DNA; ssAB, single strand abasic 11-mer DNA; DSS, 2,2-dimethyl-2-silapentane-5-sulfonic acid; DMSO, perdeuterated dimethyl sulfoxide; H bond, hydrogen bond; HSQC, heteronuclear single-quantum coherence; hUDG, human uracil DNA glycosylase; JRSE, jump-return spin-echo; LBHB, low-barrier hydrogen bond; LR-HSQC, long-range heteronuclear single-quantum coherence; MALDI-TOF, matrix-assisted laser desorption ionization time-of-flight; NMR, nuclear magnetic resonance; NOESY, nuclear Overhauser effect spectroscopy; ppm, parts per million; SSHB, short strong hydrogen bond.

temperature was calibrated as described (*26*). Data were processed on a Silicon Graphics workstation using the NMRPipe computer program (*30*). Data in the ^{13}C and ^{15}N dimensions of HSQC and LR-HSQC experiments were extended 2-fold using the standard linear prediction routine in NMRPipe.

2D NMR Experiments. The 2D NOESY experiment (*31*) was collected on the DRX 600 at 34 °C with 109 complex points and an acquisition time of 7.0 ms in t_1 and 1024 complex points and a 66 ms acquisition time in t_2. The 2D ^1H-^{15}N HSQC experiment (*32*) was collected on the DRX 500 at 25 °C with 64 complex points and an acquisition time of 3.2 ms in t_1 and 1024 complex points and an 85 ms acquisition time in t_2. The 2D ^1H-^{15}N LR-HSQC experiment was performed using the ^1H-^{15}N HSQC pulse sequence (*32*), with a de/rephasing delay of 22 ms such that signals from the weak $^2J_{NH}$ couplings in the imidazole were observed, and signals from one-bond $^1J_{NH}$ amide couplings were suppressed (*17*, *33*). The LR-HSQC experiment was collected on the DRX 600 at 34 °C with 25 complex points and a 3.4-ms acquisition time in t_1 and 512 complex points and an 85 ms acquisition time in t_2. The sample for all of these experiments contained 0.3 mM uniformly ^{15}N-labeled UDG, 0.35 mM duplex AB DNA (dsAB), 0.9 mM uracil, 150 mM NaCl, 10 mM NaH_2PO_4 at pH 10, and 7% (vol/vol) DMSO-d_6.

The 2D ^1H-^{13}C LR-HSQC spectra (data not shown) were collected using a conventional HSQC pulse sequence (*32*) with the de/rephasing delay set to 10.8 ms to eliminate signals from $^1J_{CH}$ couplings involving natural abundance ^{13}C at C5 and C6 of uracil. The spectra were recorded with 64 and 1024 complex points in t_1 and t_2 and acquisition times of 5.1 and 146 ms in t_1 and t_2, respectively.

D/H Fractionation Factor. The equilibrium D/H fractionation factor (ϕ) was determined using ^1H NMR jump-return spin-echo (JRSE) experiments (*31*) on samples with differing mole fractions of H_2O (0.17, 0.29, 0.46, 0.58, 0.71, 0.86, and 1.00). The final 0.535-mL samples contained 0.33 mM UDG, 0.44 mM dsAB, 0.52 mM uracil, 3.5 mM NaH_2PO_4 (pH 7.5), 140 mM NaCl, and 6.5% (vol/vol) DMSO-d_6. These samples were made by adding 50 μL of concentrated UDG (dissolved in 10 mM NaH_2PO_4 and 1 M NaCl in H_2O) and 33 μL of concentrated dsAB-uracil (dissolved in 40 mM NaH_2PO_4 and 0.76 M NaCl in H_2O) to 417 μL of various H_2O-D_2O mixtures. The mole fraction H_2O in each sample was calculated by weighing the addition of each component, using the known densities for H_2O and D_2O as described (*26*). Finally, 35 μL of DMSO-d_6 was added to each sample for frequency lock. The samples were placed in identical 5-mm NMR tubes (Wilmad 535-PP, Buena, NJ) and sealed with Parafilm. The JRSE experiments were collected at 25 °C on the DRX600 with 8k complex points and a 506 ms acquisition time and were processed with 10-Hz line broadening. Identical experiment parameters were used for each mole fraction H_2O sample (*26*). The integral of the His187 $H^{\epsilon 2}$ resonance, at each mole fraction H_2O [$I(X)$, eq 2] was determined by the cut and weigh method (*26*) and was plotted as a function of the mole fraction H_2O (X) and fitted to eq 2, where I^{max} is the integral at $X = 1$.

$$I(X) = (I^{max}X)/(\phi(1 - X) + X) \quad (2)$$

Although the solvent exchange rate of the His187 $H^{\epsilon 2}$ proton indicates that this proton reaches equilibrium with solvent protons at a rapid rate (8 s^{-1} at 25 °C, see text), this was confirmed by comparing the His187 $H^{\epsilon 2}$ peak integral for the 71.1 and 100% H_2O samples when the experiments were repeated after 12 and 24 h, respectively (standard deviation < 1.6%).

Temperature Dependence of the Longitudinal and Transverse Relaxation Rates. The temperature dependence of the apparent transverse relaxation rate ($1/T_{2app}$) was determined from the line width at half-height ($\Delta\nu_{1/2}$) of the His187 $H^{\epsilon 2}$ resonance using ^1H NMR spectra recorded with a JRSE pulse sequence (*31*) (eq 3). The NMR experiments were collected on the DRX 600 with 4096 complex points and a 244.2 ms acquisition time.

$$1/T_{2app} = \pi\Delta\nu_{1/2} \quad (3)$$

The temperature dependence of the longitudinal relaxation rate ($1/T_{1app}$) of the His187 $H^{\epsilon 2}$ proton was determined from ^1H NMR selective saturation recovery experiments (*34*). The His187 $H^{\epsilon 2}$ resonance was selectively saturated with a 93-Hz field strength during the 1-s recycle delay, followed by a variable recovery delay (τ), and then the conventional JRSE pulse sequence (*31*). The experiments were collected on the DRX 500 with 4096 complex points and a 272.8-ms acquisition time and were processed with 20-Hz line broadening. The $1/T_{1app}$ values were determined by fitting the integral of the His187 $H^{\epsilon 2}$ resonance (I) as a function of τ to eq 4:

$$I(\tau) = I_o(1 - \exp(-\tau/T_{1app}) \quad (4)$$

where I_o is the integral at an infinite delay (*34*). The sample at pH 10 contained 0.2 mM ^{15}N-UDG, 0.5 mM dsAB, 5.3 mM uracil, 150 mM NaCl, 10 mM NaH_2PO_4, and 10% (vol/vol) DMSO-d_6. The dipolar coupling ($1/T_{xd}$) and solvent exchange (k_{ex}) contributions to $1/T_{xapp}$ (where $X = 1$ or 2) were determined by fitting the data to eq 5:

$$\ln(1/T_{xapp}) = \ln[\exp(-E_d/RT + C_d) + \exp(-E_{ex}/RT + C_{ex})] \quad (5)$$

where E_d and E_{ex} are the activation energies for the dipolar and exchange contributions to $1/T_{xapp}$, respectively, and C_d and C_{ex} are the intercepts at infinite temperature for the dipolar and exchange contributions.

Solvent Saturation Transfer Experiments. The temperature dependence of the exchange rate (k_{ex}) of the His187 $H^{\epsilon 2}$ proton was determined using ^1H NMR solvent saturation transfer experiments. The integral of the His187 $H^{\epsilon 2}$ resonance, normalized to that of an upfield methyl resonance ($\delta = -1.23$ ppm), was determined from ^1H NMR JRSE spectra recorded with and without solvent presaturation (20-Hz field strength) during the 1 s recycle delay (*35*, *36*). The data were fitted to eq 6:

$$k_{ex} = (M_o/M_{ps} - 1)(1/T_{1d}) \quad (6)$$

where M_{ps} and M_o are the normalized integrals in spectra collected with and without presaturation, and $1/T_{1d}$ is the dipolar component of the longitudinal relaxation rate determined from the temperature dependence of the $1/T_{1app}$ (Figure

7) (*36*). The JRSE experiments were collected on the DRX 500 with 4096 complex points and a 314.6-ms acquisition time and were processed with 10-Hz line broadening. The pH 7.5 sample contained 0.34 mM UDG, 0.7 mM dsAB, 1 mM uracil, 150 mM NaCl, 10 mM NaH_2PO_4, and 7% (vol/vol) DMSO-d_6.

pH Dependence of the His187 H$^{\epsilon 2}$ Resonance in the Ternary Product Complex. The pH dependence for the disappearance of the downfield resonance (15.6 ppm) in the UDG·dsAB·U complex was determined by measuring its integral, normalized to that of an upfield methyl ($\delta = -1.23$ ppm), in ^{1}H JRSE spectra collected on the DRX500 at 25 °C. The spectra were acquired with 4096 complex points and a 314.6-ms acquisition time, and were processed with 10-Hz line broadening. The pK_a for the disappearance of the ^{1}H resonance was determined by fitting the data to eq 7:

$$I(\mathrm{pH}) = I_o(10^{\mathrm{pH}\,-\,\mathrm{p}Ka})/(10^{\mathrm{pH}\,-\,\mathrm{p}Ka} + 1) \qquad (7)$$

where I_o is the limiting value of the integral at high pH. The sample contained 0.35 mM UDG, 0.5 mM dsAB, 2 mM uracil, 150 mM NaCl, 10 mM NaH_2PO_4, and 7% (vol/vol) D_2O.

pK$_a$ of the Uracil N1 in the Binary UDG·U Complex. The ^{1}H chemical shift of the His187 H$^{\epsilon 2}$ resonance in the binary UDG·U complex was determined using JRSE ^{1}H NMR experiments collected on the DRX500 at 25 °C with 4096 complex points and a 315-ms acquisition time over the pH range of 7.8 to 10. The sample contained 0.3 mM UDG, 2.0 mM uracil, 125 mM NaCl, 10 mM NaH_2PO_4, and 6% (vol/vol) D_2O. The ^{13}C chemical shift of the uracil C2 resonance in the UDG·U complex was determined using the 2D ^{1}H-^{13}C LR-HSQC experiment as described above. The sample contained 1.2 mM UDG, 1.0 mM [^{13}C]-2-labeled uracil, 200 mM NaCl, 10 mM NaH_2PO_4, and 10% (vol/vol) D_2O. The pK_a for ionization at uracil N1 was determined by fitting the pH-dependent chemical shifts to eq 8:

$$\delta = (\delta_1 + \delta_2 10^{\,\mathrm{pH}-\mathrm{p}Ka})/(10^{\,\mathrm{pH}-\mathrm{p}Ka} + 1) \qquad (8)$$

where δ_1 and δ_2 are the limiting chemical shifts at low and high pH, respectively.

RESULTS

Low Field Proton Resonance in UDG Product Complexes with Uracil. The ^{1}H NMR spectrum of UDG in the product complex with uracil and duplex dsAB DNA at pH 7.5 reveals an unusually downfield resonance at 15.6 ppm at 15 °C (Figure 2), which increases to 15.7 ppm at −2 °C (not shown). Observation of such a highly deshielded resonance indicates the presence of a short H bond in this complex (*26*). On the basis of the following observations, this downfield proton resonance was unambiguously assigned to an H bond between His187 N$^{\epsilon 2}$ and uracil O2. (i) The resonance is not observed in the ^{1}H NMR spectra of free UDG, the UDG·dsAB complex, or the H187Q·dsAB·uracil complex (Figure 2), indicating that uracil and His187 are required to form the H bond. (ii) The 2D ^{15}N-HSQC spectra of uniformly ^{15}N-labeled UDG in complex with dsAB and uracil shows that the deshielded proton is bound to a nitrogen atom that has ^{15}N chemical shift and *J* coupling expected for an imidazole nitrogen ($\delta = 176.6$ ppm, $^1J_{NH} = 90$ Hz, see Figure 3A) (*14*, *37*). (iii) The crystal structure of hUDG in complex with duplex abasic DNA and uracil shows a 2.73 Å H bond between uracil O2 and the N$^{\epsilon 2}$ imidazole nitrogen of the corresponding His-268 and the crystal structure of eUDG in complex with single strand abasic DNA and uracil shows a 2.95-Å H bond (Figure 1). (iv) The low-field resonance shows NOESY cross-peaks to two histidine ring CH protons with chemical shifts corresponding to those previously assigned to His187 (Figure 3C) (*17*).

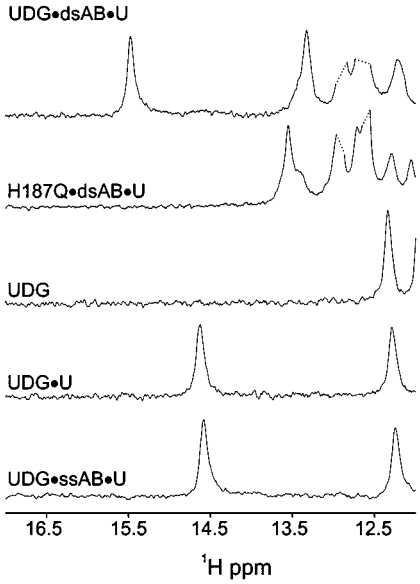

FIGURE 2: A highly downfield resonance appears in the ^{1}H NMR spectra (δ 15.5 ppm at 25 °C) of UDG in complex with duplex AB DNA and uracil (UDG·dsAB·U) but not the spectra of free UDG, H187Q·dsAB·U, or UDG·ssAB·U (not shown). A downfield resonance with a smaller chemical shift (14.6 ppm at 25 °C) appears for UDG in complex with single strand AB DNA and uracil (UDG·ssAB·U) and with uracil (UDG·U). These downfield resonances arise from the proton in an H bond between His187 and uracil O2 (see text and Figure 1). The samples contained ~0.3 mM UDG, ~0.6 mM DNA, ~2.5 mM uracil, 150 mM NaCl, 10 mM NaH_2PO_4, and 7% (vol/vol) D_2O and were at pH 10.

Although the downfield ^{1}H NMR resonance at 15.6 ppm is not observed at neutral pH for the UDG·U binary complex, or the complex of UDG with uracil and ssAB, a downfield resonance at 14.6 ppm does appear for these complexes in the pH range of ~8.5 to 10 (Figure 2). This resonance was also assigned to an H bond between His187 N$^{\epsilon 2}$ and uracil O2, on the basis of evidence similar to that described above for the UDG·dsAB·U product complex. Since this resonance is only observed at high pH values in the absence of duplex AB DNA, then these results suggest that the pK_a of uracil N1 must be higher than the value of 6.4 previously determined for the UDG·dsAB·U ternary complex (see further experiments below). The 1.0 ppm upfield shift of the H bonded proton in the UDG·ssAB·U complex as compared to the UDG·dsAB·U complex is consistent with the increased crystallographic distance for this H bond in the single stranded AB DNA complex (Figure 1).

His187 Imidazole H bond Donor is Neutral. Since the ionization state of the H bond donor and acceptor can have a significant effect on the properties of an H bond, the ionization state of His187 in the UDG·dsAB·U product complex was determined. We have recently shown using 2D ^{1}H-^{15}N long-range HSQC (LR-HSQC) experiments that

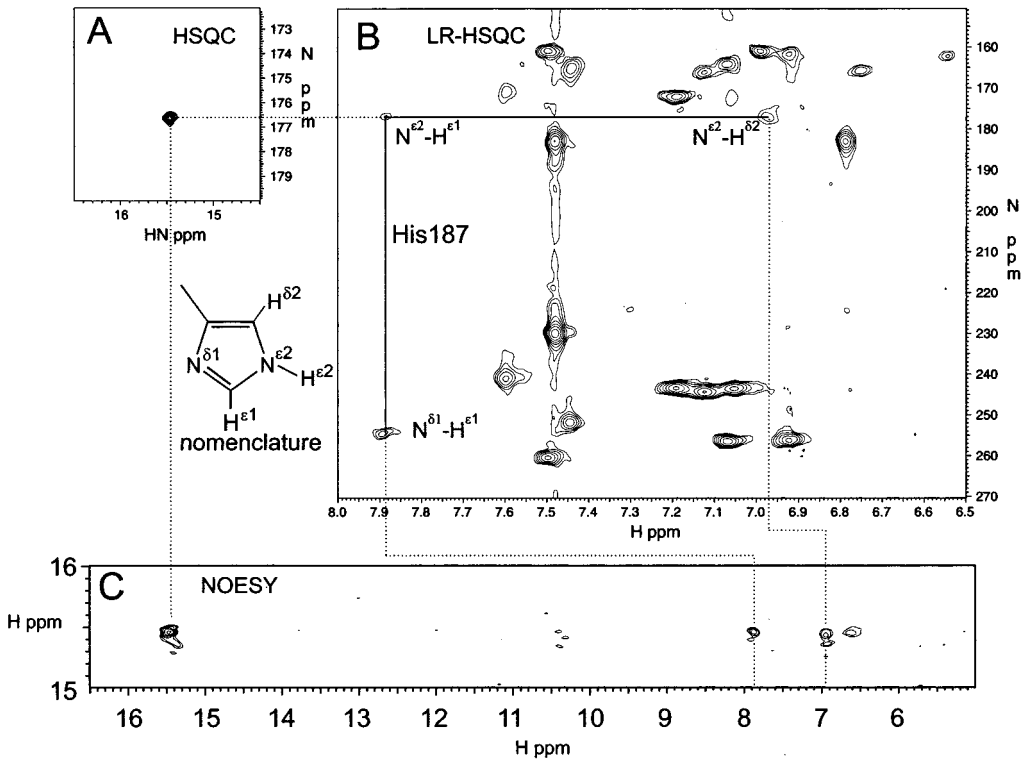

FIGURE 3: ^{15}N chemical shift and ionization state of the His187 imidazole in the UDG·dsAB·U product complex at pH 10 and 25 °C are given by the ^{1}H-^{15}N HSQC (A) and the LR-HSQC (B) spectra, respectively. Assignment of the His187 imidazole spin system in the LR-HSQC (solid lines) is on the basis of ^{15}N and ^{1}H chemical shifts from the HSQC (A) and 2D NOESY (C) spectra (dotted lines) as described in the text. The ^{15}N chemical shifts in the His187 spin system differ by 78 ppm, indicating that the imidazole is neutral (see text).

His187 is neutral in the free enzyme as well as the enzyme−substrate complex at neutral pH (pK_aE < 5.0 and pK_aES < 5.5). We used these direct NMR measurements to argue that His187 is neutral at all stages of the catalytic cycle of UDG (*17*, *18*).

Figure 3B shows the LR-HSQC spectra of uniformly ^{15}N-labeled UDG in complex with dsAB and uracil. The His187 ring spin system in this spectrum can be assigned on the basis of three observations. (i) There is only one spin system in the LRHSQC spectrum of Figure 3B with a $N^{\epsilon2}$ chemical shift corresponding to that of His187 in the HSQC spectrum (Figure 3A, 176.6 ppm). (ii) The 2D NOESY spectrum in Figure 3C shows NOE correlations from the low field proton resonance of His187 to two proton resonances with chemical shifts that correspond to the carbon bound ring protons $H^{\delta2}$ and $H^{\epsilon1}$ of the spin system labeled His187 in the LR-HSQC spectrum. (iii) The chemical shifts of $H^{\delta2}$ and $H^{\epsilon1}$ of the His187 (Figure 3C) are close to those observed for His187 in the free enzyme and the ES complex (*17*).

The two imidazole nitrogens of His187 in the product complex have ^{15}N chemical shifts of 176.6 and 254.6 ppm, indicating that His187 is neutral in the product complex, as found previously for the free enzyme and ES complex (*37*) (*17*). In addition, the peak pattern of the His187 spin system in the LR-HSQC shows that His187 is in the $N^{\epsilon2}$-H tautomeric form, as it was in the ES complex (*17*). The ^{15}N shift of the donor nitrogen shows a large 9.9 and 14.3 ppm downfield shift as compared to the free enzyme and ES complex, respectively, which indicates the formation of a shorter and stronger H bond in the product complex (*38*).

H bond Requires Negative Charge on Uracil O2. A pH titration of the UDG·dsAB·U complex using ^{1}H NMR

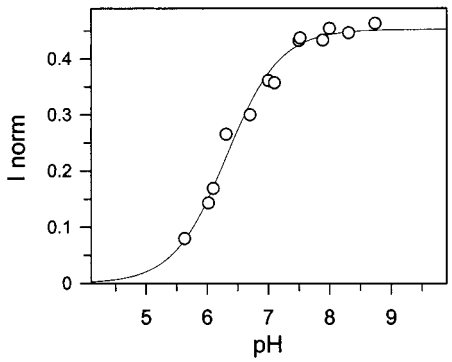

FIGURE 4: Downfield ^{1}H NMR peak (15.6 ppm) disappears with an apparent pK_a = 6.3 ± 0.1 for the UDG·dsAB·U product complex. The integral of the His187 $H^{\epsilon2}$ resonance was normalized to that of a methyl group (δ = −1.23 ppm) since the UDG concentration changed slightly during the pH titration.

revealed that the resonance at 15.6 ppm disappears with an apparent pK_a = 6.3 ± 0.1 (Figure 4). This pK_a matches the pK_a = 6.4 ± 0.1 we recently measured for dissociation of the N1 proton of uracil in the same complex, which established that uracil is bound in the N1-O2 imidate form at neutral pH (*22*). The excellent agreement of the apparent pK_a for disappearance of the H-bonded proton resonance with the pK_a for removal of the N1 proton indicates that the formation of the H bond is coupled to the formation of the uracil anion.

We also determined the pK_a for uracil N1 in the binary UDG·U complex by following the ^{13}C chemical shift of [^{13}C]-2-labeled uracil as a function of pH using the ^{13}C-LR-HSQC experiment, as previously described for the ternary product complex (*22*). As shown in Figure 5, the C2 chemical

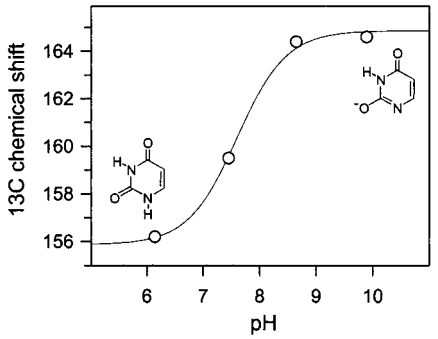

FIGURE 5: Change in ^{13}C chemical shift of uracil C2 in the binary UDG·U complex as a function of pH. A pK_a = 7.6 ± 0.1 for ionization at N1 of enzyme-bound uracil was obtained from a fit to eq 8.

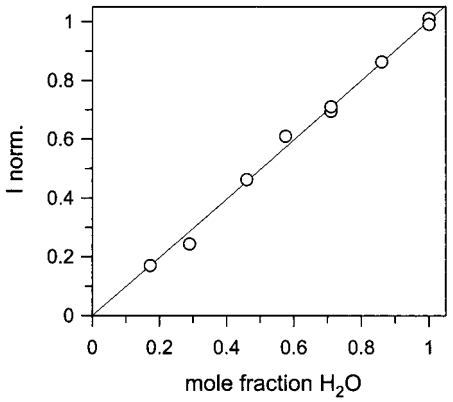

FIGURE 6: Determination of the equilibrium D/H fractionation factor (ϕ) for the His187 H$^{\epsilon 2}$ proton in the UDG·dsAB·U product complex at pH 7.5 and 25 °C. The normalized integral of the His187 H$^{\epsilon 2}$ resonance as a function of the mol fraction H_2O was fitted to eq 2 to give ϕ = 1.02 ± 0.06.

shift of bound uracil changes from a value of 156 ppm at low pH, to a limiting value of 165 ppm at high pH with an apparent pK_a of 7.6 ± 0.1. These changes are consistent with the removal of the N1 proton and generation of the N1-O2 imidate form of the uracil anion (*22*).[3] A similar pK_a = 7.5 ± 0.1 was obtained by following the His187 H$^{\epsilon 2}$ chemical shift as a function of pH, although we could not follow this chemical shift change to its endpoint at low pH due to rapid solvent exchange of the proton as the H bond is disrupted (not shown). Thus, the N1 pK_a for uracil in the binary complex is 2.2 log units lower than free uracil, but is 1.2 units higher than previously measured for uracil in the ternary product complex (*22*).

D/H Fractionation Factor for His187-H$^{\epsilon 2}$. The ϕ value for the H bond between His187 and uracil O2 in the UDG·dsAB·U product complex at pH 7.5 was determined using the ^1H JRSE NMR experiment on seven samples with differing H_2O/D_2O ratios (Figure 6). The normalized intensity of the His187 H$^{\epsilon 2}$ resonance as a function of the mole fraction H_2O of the solvent was plotted and fitted to eq 2, from which a value of ϕ = 1.02 ± 0.06 was determined.

Solvent Exchange Rate of the His187-H$^{\epsilon 2}$ Proton. The exchange rate of the His187 H$^{\epsilon 2}$ proton was determined from

[3] In the ternary complex, the observed ^{13}C chemical shift changes of uracil C2 were in the slow exchange regime, which differs from the fast exchange titration observed for the binary complex in Figure 5A (*22*). Thus, the presence of duplex DNA has a profound effect on the exchange rate of the proton at N1.

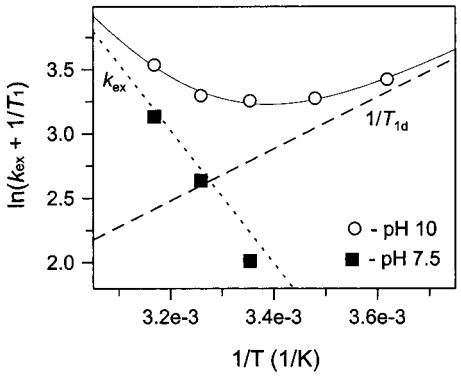

FIGURE 7: Exchange rate of the His187 H$^{\epsilon 2}$ proton (15.6 ppm) in the UDG·dsAB·U complex was determined at pH 7.5 (■) and pH 10 (○) by ^1H NMR experiments. An Arrhenius plot shows the temperature dependence of the apparent longitudinal relaxation rate ($1/T_{1app}$) at pH 10 (○), which has contributions from exchange (k_{ex}, ···) and dipolar relaxation ($1/T_{1d}$, - - -) as given by eq 5. The temperature dependence of the exchange rate was also determined using solvent saturation transfer experiments at pH 7.5 (■). A fit of the $1/T_{1app}$ data to eq 5, using E_d = −16.7 ± 1.5 kJ/mol as determined from the temperature dependence of $1/T_{2app}$ (not shown, see text), gives E_{ex} = 43.3 ± 5.9 kJ/mol, C_{ex} = 19.6 ± 2.3, and C_d = −3.9 ± 0.1.

Table 1: Properties of the H Bond from His187-N$^{\epsilon 2}$ to Uracil O2 in UDG·dsAB·U at 25 °C

				activation parameters			
δ ^1H (ppm)	(ϕ)	k_{ex} (s^{-1})	protection factor[a]	E_a (kJ/mol)	$\Delta H^‡$ (kJ/mol)	$-T\Delta S^‡$ (kJ/mol)	$\Delta G^‡$ (kJ/mol)
15.6	1.0 ± 0.1	7[b] 9[c]	400[b] 10^{5c}	43 ± 6	40 ± 6	−28	68

[a] The protection factors (k_{int}/k_{ex}) were calculated according as described in ref *59*. [b] At pH 7.5. [c] At pH 10.

the temperature dependence of the apparent longitudinal relaxation rate ($1/T_{1app}$) using a selective saturation recovery experiment. In the presence of solvent exchange, the observed $1/T_{1app}$ is the sum of the dipolar relaxation component ($1/T_{1d}$), which depends on molecular tumbling and an exchange component (k_{ex}). The contributions of these two components may be resolved experimentally because they have opposite temperature dependencies: the dipolar component decreases with increasing temperature, and the exchange component increases with increasing temperature. As shown in Figure 7, the $1/T_{1app}$ values decreased as the temperature increased from 5 to 25 °C, indicating a predominant dipolar contribution over this temperature range. However, $1/T_{1app}$ increased with temperature over the range of 25 to 43 °C, indicating an exchange contribution. Fitting the data in Figure 7 to eq 5 yields an activation energy for the exchange contribution to $1/T_{1app}$ of E_{ex} = 43 ± 6 kJ/mol. Since E_d is not well-defined by the data in Figure 7, the well-determined dipolar contribution obtained from the temperature dependence of $1/T_{2app}$ (E_d = −16.7 ± 1.5 kJ/mol, data not shown) was used during the fitting to decrease the uncertainty in the fitted value for the exchange contribution to $1/T_{1app}$. The activation parameters for exchange are given in Table 1.

To examine the effect of pH, we also determined the exchange rate at pH 7.5 using solvent saturation transfer experiments (Figure 7, squares). The exchange rate of 7 s^{-1} determined at pH 7.5 is similar to the value of 9 s^{-1} determined at pH 10, indicating that the exchange rate is

Scheme 1

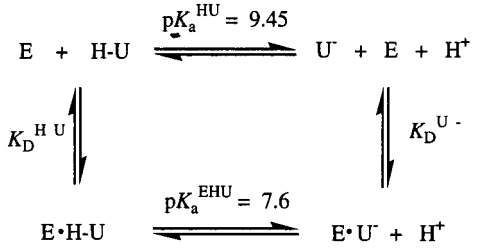

independent of pH. The calculated protection factors for this proton at pH 7.5 and pH 10 are 400 and 10^5, respectively, as determined using the pH corrected k_{int} values for neutral imidazole of 3100 and 10^6 s^{-1} (*59*).

pH dependence of Uracil Binding. Since the data indicated that formation of the short H bond required a negative charge on the uracil base (Figures 4 and 5), we sought to evaluate the energetic contribution of this negative charge to the free energy of uracil binding. Thus, the pH dependence of uracil binding to UDG was studied over the pH range 6.5 to 10.5. Due to ionization of free and enzyme-bound uracil over this pH range, the equilibrium in Scheme 1 must be considered.

At pH values much lower than the pK_a values for free and enzyme-bound uracil (pK_a^{HU} and pK_a^{EHU}, respectively), the binding equilibrium will reflect the affinity of neutral uracil (H-U) for the enzyme (K_D^{HU}). At pH values greater than pK_a^{HU} and pK_a^{EHU}, the binding equilibrium will reflect the affinity of the uracil anion for the enzyme (K_D^{U-}). At all intermediate pH values, the apparent dissociation constant (K_D^{app}) will depend on all four equilibria in Scheme 1 according to eq 9:

$$\log K_D^{app} = \log [K_D^{U-}(1 + 10^{pK_a^{HU} - pH})] - \log(1 + 10^{pK_a^{EHU} - pH}) \quad (9)$$

To determine K_D^{HU} and K_D^{U-} we take advantage of the significant change in UDG tryptophan (Trp) fluorescence that occurs upon uracil binding. Figure 8A shows that the Trp fluorescence of UDG decreases by 1.9-fold upon binding uracil at pH 10 and 25 °C, and the data can be fit to an apparent dissociation constant of $K_D^{app} = 2.1 \pm 0.3$ μM. We also determined K_D^{app} at several other pH values in the range of 6.5 to 10.5, and these values are plotted in Figure 8B as a function of pH. The data of Figure 8B were fitted to eq 9, from which values for $K_D^{HU} = 420 \pm 164$ μM and K_D^{U-} 1.9 $\pm$ 0.7 μM were determined. Since the uracil anion exists as a ~1:1 mixture of the N1 and N3 tautomers, and only the N1 tautomer is likely to bind with high affinity based on the active site structure (Figure 1), then K_D^{U-} overestimates the true K_D^{U-} by a factor of 2 (i.e., K_D^{U-} (true) = 1.9/2 = 0.95 ± 0.7 μM). Therefore, the affinity of UDG for the uracil N1 anion is over 400-fold greater than the neutral species.

To estimate the energetic contribution of the H bond between His187 and the uracil O2 anion to binding, the uracil binding measurements were repeated with the H187G mutant at pH 10 (square, Figure 8B). As compared to the wild-type enzyme, a 43-fold larger K_D value of 81 ± 5 μM is observed. Other methods for estimating the strength of this H bond are discussed below.

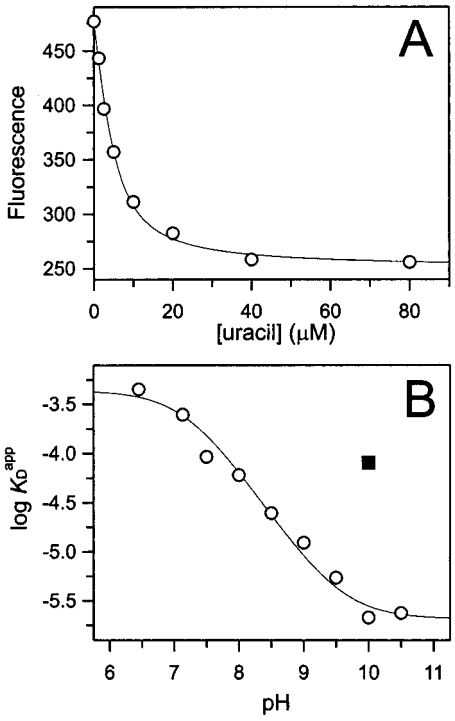

FIGURE 8: (A) Apparent dissociation constant (K_D^{app}) for the binding of uracil to UDG at pH 10 was determined by monitoring the change in the UDG tryptophan fluorescence at 330 nm as a function of total uracil concentration. The line shows the best fit of the data to eq 1 by nonlinear regression, which gives $K_D^{app} = 2.1 \pm 0.3$ μM. (B) The pH of the dependence of the binding of uracil to wild-type UDG (○) and the H187G mutant (■) at pH 10. The line shows the best fit of the data to eq 9, which gives p$K_a^{HU} = 9.5 \pm 0.2$, and p$K_a^{EHU} = 7.2 \pm 0.2$.

DISCUSSION

Nature of the H bond from His187-N$^{\epsilon 2}$ to Uracil O2. NMR is perhaps the most informative experimental approach for probing the properties of H bonds in enzymes and proteins. Each of the observable NMR parameters provides a unique view into the chemical properties of the H bond under investigation.

(1) Proton Chemical Shift Implications. The unusually downfield ^{1}H chemical shift of His187 H$^{\epsilon 2}$ (δ 15.6 ppm) indicates that the H bond between His187 N$^{\epsilon 2}$ and uracil O2 in the UDG product complex is short and, therefore, relatively strong (vida infra). This conclusion is supported by experimental and theoretical studies that have established that ^{1}H chemical shift of the H bonded proton increases as the donor−acceptor distance decreases for both O-O and N-O type H bonds (*39*−*43*). There is also good evidence that correlates ^{1}H chemical shift with H bond strength. In the case of chymotrypsin/peptidyl trifluoromethyl ketone inhibitor complexes, which involve a short H bond between a cationic His57 and an anionic Asp102 of the catalytic triad, Frey and colleagues have demonstrated a linear correlation between ^{1}H chemical shift and log K_i for inhibition (*44*). Additionally, linear correlations between H bond strength and ^{1}H chemical shift have been obtained in theoretical studies of the strong H bonds between formic acid and substituted formate anions and between enol and substituted enolate anions (*9*). Thus, downfield ^{1}H chemical shifts arise from short H bonds in which the H-acceptor interaction

Table 2: Comparison of Parameters for Short H Bonds (N-O Type) in Several Enzymes and a Model Compound

enzyme or model system	interaction	R_{N-O} (Å)	δ ^{1}H (ppm)[a]	$\Delta\delta$ ^{1}H (ppm)[b]	$\Delta\delta$ ^{15}N (ppm)[c]	$^1J_{NH}$ (Hz)	D/H fract factor ϕ	k_{ex} (s^{-1}) 25 °C	ΔG_{HB} (kJ/mol)
UDG·dsAB·U[d]	His>N−H···$^-$O−C	2.73[e]	15.7 (15.6)[d]	4.3	10.9 (14.3)[d]	90	1.0	7	−20[f]
TIM·PGH[g]	His>N−H···$^-$O−C	2.66[h]	13.5	2.1	7.6	98	0.7	80[i]	−12.2[j]
serine proteases[k]									
high pH	His>N−H···$^-$OOC	2.62[h]	15.0[l,m]	3.6	10.9[l]	90[l]	0.8[m]−2.0[n]	3520[n]	
low pH	His$^+$>N−H···$^-$OOC	2.52−2.59[h]	17[l]−18[m,n]	4.8−5.8	12.0[l]	80[l]	0.4−0.7[m,n,o]	952[n]	−21[l]
TFMK complex	His$^+$>N−H···$^-$OOC		18−19[p,q]	5.8−6.8	12[r]−23[p]	81[p]	0.3−0.4[q]	12−282[q]	−29[s]
cis-urocanic acid[t]	His>N−H···$^-$OOC		15.0	3.6	14.8				−21
	His$^+$>N−H···$^-$OOC		18.5	6.3	11.0				

[a] Values at $T \leq 5$ °C except as noted. [b] The change in ^{1}H shifts are relative to 11.4 ppm for imidazole and 12.2 ppm for imidazolium in $CDCl_3$ (*60*). [c] The change in ^{15}N shifts are relative to the expected ^{15}N shifts in H_2O for a neutral imidazole in the $N^{\epsilon 2}$-H (165.7 ppm) or $N^{\delta 1}$-H (167.2 ppm) tautomeric forms or imidazolium ion ($N^{\delta 1}$ = 173.9 ppm) (*37*). The ^{15}N shifts are referenced to external liquid ammonia, and values originally referenced to 1 M HNO_3 were converted by subtracting the HNO_3 value from 377.5. [d] Values from this work. The ^{1}H shift is temperature-dependent for UDG, and the value in parentheses was determined at 15 °C. The $\Delta\delta$ ^{15}N value in parentheses is relative to the ^{15}N shift in the ES complex (see text). [e] From ref *20*. [f] Based on the $\Delta pK_a^{N1} = 3.4$ units for enzyme-bound uracil relative to free uracil (*22*). [g] For the H bond between His95 of triosephosphate isomerase (TIM) and O2 of phosphoglycohydroxamate (PGH) (*61, 62*). [h] From ref *26*. [i] At 30 °C. [j] The damaging effect of the H95Q mutation (*63*). [k] Values for the His-Asp H bond in the catalytic triad of several serine proteases as noted. [l] For α-lytic protease (*14*). [m] For chymotrypsin (*24*). [n] For chymotrypsinogen A; k_{ex} was measured at 1 °C (*64*). [o] For subtilisin Carlsberg (*46*). [p] For subtilisin Carlsberg complexed with peptidyl-(trifluromethyl ketones) (TFMKs) (*46*). [q] For chymotrypsin complexed with peptidyl-TFMKs (*44*). [r] For α-lytic protease in complex with chloromethyl ketones (*49*). [s] From $\Delta pK_a = 5.2$ for His57 imidazolium in chymotrypsin-peptidyl TMFK complexes as compared to free imidazolium (*25*). [t] Values for *cis*-urocanic acid are from ref *14* and references therein.

weakens the H-donor bond, thereby delocalizing the hydrogen and decreasing its shielding.

The ^{1}H chemical shift of the short H bond proton in the UDG product complex is compared with several other noteworthy H bonds involving imidazole donors and oxygen acceptors in Table 2. Although the ^{1}H chemical shift for UDG is not as large as that found in the low pH form of the serine proteases (~18 ppm) or the intramolecular imidazolium−carboxylate H bond in the model compound *cis*-uraconic acid (18.5 ppm), these later two interactions involve a charged donor and acceptor, whereas the UDG reaction involves a neutral donor. Thus, it is not useful to infer distances or strengths between these H bonds on the basis of the absolute values of the chemical shifts. It may be more appropriate to compare the high pH forms of these H bonds with the UDG H bond (i.e., when the donor is neutral). In this comparison, the H bond proton of UDG (15.6 ppm) has a considerably larger chemical shift than the short H bonds in the serine proteases (15.0 ppm), *cis*-uraconic acid (15.0 ppm), or the H bond between His95 of triose phosphate isomerase and the carbonyl oxygen of the bound dienolate intermediate analogue, phosphoglycohydroxymate (13.5 ppm, Table 2). To our knowledge, the 15.6 ppm chemical shift for this proton is the largest yet reported for a neutral imidazole donor and a negatively charged oxygen acceptor.

(2) ^{15}N Chemical Shift and Scalar Coupling Constant Implications. Model studies have shown that the ^{15}N chemical shift of a nitrogen H bond donor is quite sensitive to H bond strength, exhibiting an increase in chemical shift as the H bond becomes stronger and the N-H bond lengthens (*14, 38, 45*). The ^{15}N chemical shift of His187 $N^{\epsilon 2}$ is increased by 14.3 ppm in the UDG·dsAB·U complex (δ = 176.6 ppm) as compared to its value in the ES complex (162.4 ppm) (*17*). This indicates that the His187 H bond to the neutral uracil O2 carbonyl group in the ES complex is significantly weaker than the H bond to the uracil anion in the product complex (*17*) and suggests that some degree of proton transfer to uracil O2 has occurred. If the proton was fully transferred to uracil O2, an increase of 84 ppm would be expected on the basis of the 84 ppm difference in the chemical shift between an >NH type and >N: type imidazole nitrogen (*14*). The observed value of 14.3 ppm is thus consistent with about 17% proton transfer in the product complex. This extent of proton transfer is within the range of values previously calculated for the proposed LBHBs in the mechanism of serine proteases (15 to 30%) (*14, 46*).

The scalar coupling constant for the N-H bond ($^1J_{NH}$) is expected to decrease as H bond strength increases and the hydrogen−acceptor interaction strengthens, as has been shown recently by ab initio calculations on model systems (*47*) and experimentally for H bonds in DNA (*48*). However, a determination of the change in $^1J_{NH}$ upon forming the short H bond in the UDG product complex is lacking, because rapid exchange of the proton with solvent precludes a measurement of $^1J_{NH}$ in the free enzyme. Thus, it is difficult to interpret the magnitude of the $^1J_{NH}$ = 90 Hz observed for the $N^{\epsilon 2}$-H bond of His187 in the UDG product complex (Table 2). However, the expected $^1J_{NH}$ for an imidazole N-H bond is 90−100 Hz (*14*) (*49*), which suggests that the proton is localized predominantly on $N^{\epsilon 2}$ of His187, consistent with the conclusion from the nitrogen shift changes (see above).

(3) Hydrogen Exchange Properties. A strong H bond is expected to slow the solvent exchange rate (k_{ex}) of the bridging hydrogen significantly as compared to the intrinsic rate in the absence of an H bond (k_{int}), which may be expressed as a protection factor (P. F. = k_{int}/k_{ex}) (*26*). For UDG, the protection factors of 400 and 10^5 at pH 7.5 and pH 10, respectively, certainly meet this expectation. Indeed, Table 2 shows that the exchange rate for the short H bond proton in UDG is slower than that reported for any of the proposed LBHBs in ketosteroid isomerase (KSI), triosephosphate isomerase (TIM), or the serine proteases (Table 2) (*26, 44*).

The direct interpretation of these protection factors as a measure of H bond strength is complicated. This is exemplified by the general observation that backbone amide H bonds of proteins can exhibit essentially no exchange for months or longer, even though these bonds are generally weak. Thus, the mechanism of proton exchange is an important consideration. In this case, the exchange rate of His187 $H^{\epsilon 2}$ in the

ternary complex is independent of pH (Figure 7), indicating that the exchange process reflects either the microscopic energetic barrier for breakage of the H bond or another global event that leads to disruption of the H bond (*50*). A likely factor that limits the exchange rate, and is unrelated to H bond strength, is dissociation of the dsAB from the ternary product complex. The overall rate of steady-state turnover for UDG is limited by a step after glycosidic bond cleavage ($k_{cat} = 1.5\ s^{-1}$), most likely a step leading to dissociation of the DNA product (*18*). Although the NMR experiments are performed using higher ionic strength conditions than the kinetic measurements, the k_{cat} value is similar to the rate constant for exchange of the H bond proton, suggesting that exchange is limited by dsAB dissociation.

Why is the Fractionation Factor Unity? Another physicochemical property that can be useful for identifying strong H bonds is the equilibrium D/H fractionation factor (ϕ), which expresses the preference for deuterium over protium at a solute site relative to the solvent. Fractionation factors measure the "tightness" of bonding of a hydrogen in a solute site as compared to the reference oxygen−hydrogen bonds of water. A value of $\phi < 1$ indicates a solute site that has looser bonds than those of the bulk solvent, and a value of $\phi > 1$ reflects a solute site that has tighter bonding than the reference bonds of the solvent. As an H bond becomes shorter, and approaches a LBHB, the fractionation factor can decrease to a minimum of about 0.3 but then increases as the distance becomes even shorter and approaches a single well H bond (*8*, *51*).

The fractionation factor of 1.0 for the product complex of UDG is surprisingly large in light of the short crystallographic distance, and the ^1H and ^{15}N chemical shifts, both of which indicate that this H bond is short. One factor that may increase or decrease ϕ, but is unrelated to bond stretching frequency differences in the solvent and solute sites, is a change in bending frequencies accompanying H-bond formation in the solute (*52*). For instance, fractionation studies on *N*,*N*-substituted benzylammonium ions by Kresge and co-workers have shown that anomalously high ϕ values may result from compensatory increases in bond bending vibration frequencies upon H bond formation (*53*, *54*). Thus, a strong hydrogen bond that undergoes a decrease in stretching frequency as compared to solvent may have a larger than expected ϕ value because of a compensatory increase in a bending vibration frequencies. Such compensatory changes in vibrational modes may account for the observation that the backbone amide H bonds in β-sheet residues have higher fractionation factors than in α-helical residues, despite evidence that the β-sheet H bonds are shorter and stronger (*55*, *56*). Another factor that could contribute to the larger than expected fractionation factor for this H bond would be a significant pK_a mismatch between the His187 donor and the uracil O2 acceptor. The pK_a values for both of these groups are presently unknown.

How Strong is This Short H bond? The deceptively simple interaction of the H bond is one of the most problematic to dissect energetically. This problem arises even in simple model systems because H bonds energies are extremely sensitive to environment and solvent (*8*) and is even more problematic in enzymatic catalysis because such bonds are usually part of a complex and cooperative network of interactions that cannot be easily separated into discrete energetic contributions. In the section below, we describe several experimental approaches to estimate the strength of the H bond in this system (ΔG^{HB}) and then critically evaluate each approach. The limitations of estimating ΔG^{HB} in this system are no greater or less than other enzyme systems and reflect the inherent uncertainties in making such evaluations.

(1) Damaging Effect of Removing the Imidazole Side Chain of His187 on $\Delta G^{\ddagger}$ and Uracil Binding. The energetic effect of deleting an amino acid side chain can, in principle, provide information as to the strength of an H bond involving this side chain. We have previously mutated the active site His187 of eUDG to both Gln and Ala and determined that the imidazole side chain contributes little to ground-state binding but contributes about 20 kJ/mol to transition-state stabilization (*18*). Minimally, this energetic effect should be considered as the relative stabilization of this side chain as compared to the interaction with water, as the high-resolution crystal structure of the H187Q mutant indicates that solvent fulfills this interaction (*19*). However, a quantitative interpretation of this effect in terms of the H bond free energy should be made cautiously, because extensive mutagenesis studies of UDG have shown cooperative and anticooperative interactions between active site residues involved in substrate binding and catalysis (unpublished results).

Similarly, the energetic effect of the H187G mutation on uracil binding at high pH (Figure 8) should provide information as to the strength of the H bond interaction between the His187 imidazole N-H and the O2 anion of uracil in the binary complex. On the basis of the differences in the K_D^{U-} values for the wild-type and H187G mutant enzymes at pH 10, this energetic effect is 9.3 kJ/mol, which is considerably less than the effect of the H187Q mutation on catalysis (20 kJ/mol). This lesser energetic effect in the binary complex is consistent with (i) the 1 ppm upfield shift of the H bonded proton in the binary complex as compared to the ternary complex (Figure 2) and (ii) the smaller decrease in pK_a^{N1} for uracil in the binary complex as compared to the ternary complex ($\Delta pK_a = 2.2$ as compared to free uracil, corresponding to a free energy for stabilization of the anion of 12.6 kJ/mol in the binary complex) (Figure 5).

(2) Change in N1 pK_a of Uracil. In principle, the energetic contribution of an H bond can also be estimated by the decrease in pK_a of the acceptor upon formation of the H bond (*3*). Such a decrease for the ionization at uracil N1 upon formation of an H bond at O2 is observed in both the ternary and the binary product complexes of UDG and in a model system with uracil (see Figure 5) (*22*, *57*). The observed decreases in pK_a of 3.4 and 2.2 units as compared to free uracil (p$K_a^{N1} = 9.8$) correspond to 20 and 12.6 kJ/mol of stabilization energy by the enzyme (see ref *23* and citations therein). The stabilization energy of the uracil anion in the ternary complex is indistinguishable from the stabilizing effect of His187 in the transition state (see above), which suggests that the uracil interactions in the product complex are similar to the transition-state or the putative high-energy oxycarbenium ion−uracil anion intermediate. This comparison assumes that all of the stabilization energy of the uracil anion is due to the H bond between His187 $N^{\epsilon 2}$ and uracil O2. This assumption is largely supported by the observation that the binding energy of the wild-type enzyme for the uracil anion is 9.3 kJ/mol more favorable than the H187G mutant,

which is similar to the total stabilization of the uracil anion in the binary complex (12.6 kJ/mol). As shown in Table 2, the $\Delta G^{HB} = -20$ kJ/mol for the UDG system based on ΔpK_a^{N1} in the ternary complex falls within the range of estimates for the LBHB in serine proteases ($\Delta G^{HB} = -20$ to -29 kJ/mol).

(3) Correlating $\Delta\delta$ ^1H and ΔpK_a of Bound Uracil. There is a substantial body of experimental and theoretical evidence that supports the conclusion that as the length of an H bond decreases (or equivalently, the strength increases), the proton becomes more deshielded and the chemical shift increases (*39*, *40*). Theoretical studies have indicated a linear correlation between H bond energy and ^1H chemical shift for SSHBs and LBHBs in O-O donor−acceptor systems (*9*). The average slopes of these linear correlations were about 6.3 kJ $(mol)^{-1}$ $(ppm)^{-1}$, which provides a crude benchmark to address such changes in experimental systems. Thus, if a change in free energy that is related to the H bond strength can be measured experimentally, and then correlated with the corresponding change in chemical shift of the proton, then information about the steepness of the energy−distance dependence of the interaction is provided. In the present case, we have determined the chemical shift of the H bonded proton in the ternary and binary product complexes ($\Delta\delta =$ 1 ppm), and we have also determined the difference in pK_a for uracil N1 in these two complexes ($\Delta pK_a = 1.2$). From these values, an energy−chemical shift dependence of 6.9 kJ mol^{-1} ppm^{-1} is obtained ($= -2.303\ RT\ \Delta pK_a/\Delta\delta$), which is consistent with a strong interaction on the basis of the benchmark value of 6.3 kJ mol^{-1} ppm^{-1} from theoretical studies. The assumptions in the above analysis are that (i) the gradient determined for the O-O type SSHB is a reasonable approximation for N-O type H bond, (ii) that a linear correlation holds outside the range of 2.42 to 2.64 Å, and most importantly (iii) that the structures for the binary and ternary complexes have identical functional interactions with the uracil base that lead to the changes in pK_a^{N1}, H bond distance, and proton chemical shift. Although these assumptions appear reasonable, this final estimate of H bond strength must also be interpreted cautiously.

Catalytic Significance. The fundamental observation from these studies, which was entirely unexpected from the crystal structures of UDG (*19*, *20*), is that the enzyme active site is constructed to significantly stabilize the uracil anion such that it exists as a stable species at neutral pH. This observation suggests several catalytic advantages. First, the significant energetic problem of activating the uracil leaving group by protonating a carbonyl oxygen ($pK_a < -3$) is circumvented by forming an H bond with uracil O2 that becomes strong only as charge develops at this position. This is an excellent example of a preorganized active site that solvates developing charge in the transition state without forming strong interactions in the ground state. Second, providing an active site environment that lowers the pK_a of the leaving group by at least 3.4 units (as estimated from pK_a^{N1} in the product complex), would be expected to result in a $10^{3.4}$-fold increase in the rate, on the basis of the $\beta_{lg} \sim -1$ for the uncatalyzed hydrolysis of 5-halogen-substituted deoxyuridine derivatives (*23*). (The β_{lg} value is the slope of a plot of log rate versus pK_a^{N1} of the uracil leaving group; a value of -1 indicates a late transition state for the solution reaction in which a full negative charge has developed on the uracil base.) If β_{lg} in the enzyme active site is comparable, then a similarly strong rate enhancement could be realized by lowering pK_a^{N1} of uracil. Third, we currently have strong evidence, on the basis of competitive isotope effect measurements, that the UDG reaction proceeds through a very late transition state with a large amount of oxycarbenium ion character or perhaps even a discrete oxycarbenium ion intermediate (*58*). Since there are few groups in the UDG active site that appear to be candidates for stabilizing such an intermediate, it is attractive to suggest that the uracil anion itself serves this function. According to the proposed mechanisms for purine DNA glycosylases and purine *N*-ribohydrolase enzymes, such "product-assisted" catalysis is not possible because the purine leaving group is assumed to be protonated before bond cleavage. Thus, pyrimidine specific DNA glycosylases may have evolved a single mechanism to stabilize both the leaving group anion and the cationic sugar.

REFERENCES

1. Warshel, A. (1998) *J. Biol. Chem. 273*, 27035−27038.
2. Cannon, W. R., and Benkovic, S. J. (1998) *J. Biol. Chem. 273*, 26257−26260.
3. Shan, S. O., Loh, S., and Herschlag, D. (1996) *Science 272*, 97−101.
4. Cleland, W. W., Frey, P. A., and Gerlt, J. A. (1998) *J. Biol. Chem. 273*, 25529−25532.
5. Gerlt, J. A., and Gassman, P. G. (1993) *J. Am. Chem. Soc. 115*, 11552−11568.
6. Cleland, W. W., and Kreevoy, M. M. (1994) *Science 264*, 1887−1890.
7. Frey, P. A., Whitt, S. A., and Tobin, J. B. (1994) *Science 264*, 1927−1930.
8. Hibbert, F., and Emsley, J. (1990) *Adv. Phys. Organ. Chem. 26*, 255−379.
9. Kumar, G. A., and McAllister, M. A. (1998) *J. Org. Chem. 63*, 6968−6972.
10. Warshel, A., Papazyan, A., and Kollman, P. A. (1995) *Science 269*, 102−106.
11. Warshel, A., and Papazyan, A. (1996) *Proc. Natl. Acad. Sci. U.S.A. 93*, 13665−13670.
12. Guthrie, J. P. (1996) *Chem. Biol. 3*, 163−170.
13. Scheiner, S., and Kar, T. (1995) *J. Am. Chem. Soc. 117*, 6970−6975.
14. Ash, E. L., Sudmeier, J. L., De Fabo, E. C., and Bachovchin, W. W. (1997) *Science 278*, 1128−1132.
15. Guthrie, J. P., and Kluger, R. (1993) *J. Am. Chem. Soc. 115*, 11569−11572.
16. Alagona, G., Ghio, C., and Kollman, P. A. (1995) *J. Am. Chem. Soc. 117*, 9855−9862.
17. Drohat, A. C., Xiao, G., Tordova, M., Jagadeesh, J., Pankiewicz, K. W., Watanabe, K. A., Gilliland, G. L., and Stivers, J. T. (1999) *Biochemistry 38*, 11876−11886.
18. Drohat, A. C., Jagadeesh, J., Ferguson, E., and Stivers, J. T. (1999) *Biochemistry 38*, 11866−11875.
19. Xiao, G., Tordova, M., Jagadeesh, J., Drohat, A. C., Stivers, J. T., and Gilliland, G. L. (1999) *Proteins 35*, 13−24.
20. Parikh, S. S., Mol, C. D., Slupphaug, G., Bharati, S., Krokan, H. E., and Tainer, J. A. (1998) *EMBO J. 17*, 5214−5226.
21. Stivers, J. T., Pankiewicz, K. W., and Watanabe, K. A. (1999) *Biochemistry 38*, 952−963.
22. Drohat, A. C., and Stivers, J. T. (2000) *J. Am. Chem. Soc. 122*, 1840−1841.
23. Shapiro, R., and Kang, S. (1969) *Biochemistry 8*, 1806−1810.
24. Bao, D. H., Huskey, W. P., Kettner, C. A., and Jordan, F. (1999) *J. Am. Chem. Soc. 121*, 4684−4689.
25. Cassidy, C. S., Lin, J., and Frey, P. A. (1997) *Biochemistry 36*, 4576−4584.

26. Mildvan, A. S., Harris, T. K., and Abeygunawardana, C. (1999) *Methods Enzymol. 308*, 219−245.
27. Birdsall, B., King, R. W., Wheeler, M. R., Lewis, C. A., Goode, S. R., Dunlap, R. B., and Roberts, G. C. K. (1983) *Anal. Biochem. 132*, 353−361.
28. Leatherbarrow, R. J. (1998) *GraFit 4.0*, Erithacus Software Ltd., Staines, U.K.
29. Wishart, D. S., Bigam, C. G., Yao, J., Abildgaard, F., Dyson, H. J., Oldfield, E., Markley, J. L., and Sykes, B. D. (1995) *J. Biomol. NMR 6*, 135−140.
30. Delaglio, F., Grzesiek, S., Vuister, G. W., Zhu, G., Pfeifer, J., and Bax, A. (1995) *J. Biomol. NMR 6*, 277−293.
31. Sklenar, V., and Bax, A. (1987) *J. Magn. Reson. 74*, 469−479.
32. Mori, S., Abeygunawardana, C., Johnson, M. O., and van Zijl, P. C. (1995) *J. Magn. Reson. B. 108*, 94−98.
33. Pelton, J. G., Torchia, D. A., Meadow, N. D., and Roseman, S. (1993) *Protein Sci. 2*, 543−558.
34. Freeman, R. (1997) in *A Handbook of Nuclear Magnetic Resonance*, Addison-Wesley Longman, Essex.
35. Rosevear, P. R., Fry, D. C., and Mildvan, A. S. (1985) *J. Magn. Reson. 61*, 102−115.
36. Spera, S., Ikura, M., and Bax, A. (1991) *J. Biomol. NMR 1*, 155−165.
37. Farrjones, S., Wong, W. Y. L., Gutheil, W. G., and Bachovchin, W. W. (1993) *J. Am. Chem. Soc. 115*, 6813−6819.
38. Bachovchin, W. W. (1986) *Biochemistry 25*, 7751−7759.
39. McDermott, A., and Ridenour, C. F. (1996) in *Encyclopedia of Nuclear Magnetic Resonance* (Grant, D. M., and Harris, R. K., Eds.) pp 3820, John Wiley, Sussex.
40. Bertolasi, V., Gilli, P., Ferretti, V., and Gilli, G. (1997) *J. Chem. Soc.-Perkin. Trans. 2*, 945−952.
41. Wagner, G., Pardi, A., and Wuthrich, K. (1983) *J. Am. Chem. Soc. 105*, 5948−5949.
42. Wishart, D. S., Sykes, B. D., and Richards, F. M. (1991) *J. Mol. Biol. 222*, 311−333.
43. Li, H., Yamada, H., and Akasaka, K. (1998) *Biochemistry 37*, 1167−1173.
44. Lin, J., Westler, W. M., Cleland, W. W., Markley, J. L., and Frey, P. A. (1998) *Proc. Natl. Acad. Sci. U.S.A. 95*, 14664−14668.
45. Benedict, H., Limbach, H. H., Wehlan, M., Fehlhammer, W. P., Golubev, N. S., and Janoschek, R. (1998) *J. Am. Chem. Soc. 120*, 2939−2950.
46. Halkides, C. J., Wu, Y. Q., and Murray, C. J. (1996) *Biochemistry 35*, 15941−15948.
47. Benedict, H., Shenderovich, I. G., Malkina, O. L., Malkin, V. G., Denisov, G. S., Golubev, N. S., and Limbach, H.-H. (2000) *J. Am. Chem. Soc. 122*, 1979−1988.
48. Dingley, A. J., Masse, J. E., Peterson, R. D., Barfield, M., Feigon, J., and Grzesiek, S. (1999) *J. Am. Chem. Soc. 121*, 6019−6027.
49. Tsilikounas, E., Rao, T., Gutheil, W. G., and Bachovchin, W. W. (1996) *Biochemistry 35*, 2437−2444.
50. Englander, S. W., and Kallenbach, N. R. (1983) *Q. Rev. Biophys. 16*, 521−655.
51. Kreevoy, M., and Liang, T. (1980) *J. Am. Chem. Soc. 102*, 3315−3322.
52. Edison, A. S., Weinhold, F., and Markley, J. L. (1995) *J. Am. Chem. Soc. 117*, 9619−9624.
53. Arrowsmith, C. H., Guo, H. X., and Kresge, A. J. (1994) *J. Am. Chem. Soc. 116*, 8890−8894.
54. Guo, H. X., and Kresge, A. J. (1997) *J. Chem. Soc.-Perkin. Trans. 2*, 295−298.
55. Bowers, P. M., and Klevit, R. E. (2000) *J. Am. Chem. Soc. 122*, 1030−1033.
56. Cordier, F., and Grzesiek, S. (1999) *J. Am. Chem. Soc. 121*, 1601−1602.
57. Kimura, E., Kitamura, H., Koike, T., and Shiro, M. (1997) *J. Am. Chem. Soc. 119*, 10909−10919.
58. Werner, R. M., and Stivers, J. T., submitted for publication.
59. Connelly, G. P., Bai, Y., Jeng, M.-F., and Englander, S. W. (1993) *Proteins 17*, 87−92.
60. Clark, J. H., Green, M., and Madden, R. G. (1983) *J. Chem. Soc. Chem. Commun.* 136−137.
61. Harris, T. K., Abeygunawardana, C., and Mildvan, A. S. (1997) *Biochemistry 36*, 14661−14675.
62. Lodi, P. J., and Knowles, J. R. (1991) *Biochemistry 30*, 6948−6956.
63. Nickbarg, E. B., Davenport, R. C., Petsko, G. A., and Knowles, J. R. (1988) *Biochemistry 27*, 5948−5960.
64. Markley, J. L., and Westler, W. M. (1996) *Biochemistry 35*, 11092−11097.

BI000922E